

# Resolved photon and multi-component model for $\gamma^*p$ and $\gamma^*\gamma^*$ scattering at high energies

T. Pietrycki <sup>1</sup> and A. Szczurek <sup>1,2</sup>

<sup>1</sup> *Institute of Nuclear Physics  
PL-31-342 Cracow, Poland*

<sup>2</sup> *University of Rzeszów  
PL-35-959 Rzeszów, Poland*

## Abstract

We generalize our previous model for  $\gamma^*p$  scattering to  $\gamma\gamma$  scattering. In the latter case the number of components naturally grows. When using the model parameters from our previous  $\gamma^*p$  analysis the model cross section for  $\gamma\gamma$  scattering is larger than the corresponding LEP2 experimental data by more than a factor of two. However, performing a new simultaneous fit to  $\gamma^*p$  and  $\gamma\gamma$  total cross section we can find an optimal set of parameters to describe both processes. We propose new measures of factorization breaking for  $\gamma^*\gamma^*$  collisions and present results for our new model.

## 1 Introduction

In the last decade the photon-proton and photon-photon reactions became a testing ground for different QCD-inspired models. The dipole model was one of the most popular and successful in this respect. In the simplest version of the model only quark-antiquark Fock components of the photon are included in order to describe the total cross sections. In contrast, the more exclusive processes, like diffraction [1], jet [2] or heavy quark [3] production, require inclusion of higher Fock components of the photon. The higher Fock components can be of both perturbative and nonperturbative nature, and therefore are rather difficult to include in a systematic manner.

In our recent publication [4] we have constructed a simple hybrid model which includes the resolved photon component in addition to the quark-antiquark component. With a very small number of parameters we were able

to describe the HERA  $\gamma^*p$  total cross section data with an accuracy similar to that of very popular dipole models [5, 6, 7, 8, 9]. The advantage of our model is that it treats the total cross section and the exclusive processes on the same footing.

The notion of the resolved photon is general and applies not only to photon-proton collisions. In the present paper we shall try to generalize our hybrid model also to photon-photon collisions. Our approach is similar in the spirit to the approach of Ref.[10] although the details differ considerably.

## 2 Formulation of the model

### 2.1 $\gamma^*p$ scattering

First, let us recall our model for the total cross section for  $\gamma^*p$  collisions. In this model the total cross section is a sum of three components,

$$\sigma_{\gamma^*N}^{tot}(W, Q^2) = \sigma_{dip}^{tot}(W, Q^2) + \sigma_{VDM}^{tot}(W, Q^2) + \sigma_{val}^{tot}(W, Q^2) \quad (1)$$

where:

$$\sigma_{dip}^{tot}(W, Q^2) = \sum_q \int dz \int d^2\rho \sum_{T,L} \left| \Psi_{\gamma^* \rightarrow q\bar{q}}^{T,L}(Q, z, \rho) \right|^2 \cdot \sigma_{(q\bar{q})N}(x, \rho) \quad (2)$$

and

$$\sigma_{VDM}^{tot}(W, Q^2) = \sum_V \frac{4\pi}{\gamma_V^2} \frac{M_V^4 \sigma_{tot}^{VN}(W)}{(Q^2 + M_V^2)^2} \cdot (1-x). \quad (3)$$

All components of our model are illustrated graphically in Fig.1. The last component becomes important only at large  $x$ , i.e. small  $W$ .

We take the simplest diagonal version of VDM with  $\rho$ ,  $\omega$  and  $\phi$  mesons included. As discussed recently in Ref.[11] the contributions of higher vector states are expected to be damped. Above the meson-nucleon resonances it is reasonable to approximate

$$\sigma_{tot}^{\rho N}(W) = \sigma_{tot}^{\omega N}(W) = \frac{1}{2} \left[ \sigma_{tot}^{\pi^+ p}(W) + \sigma_{tot}^{\pi^- p}(W) \right], \quad (4)$$

with a similar expression for  $\sigma_{\phi p}^{tot}$  [12]. A simple Regge parametrization of the experimental pion-nucleon cross section by Donnachie and Landshoff is used [13]. As in Ref. [12] we take  $\gamma$ 's calculated from the leptonic decays of vector mesons, including finite width corrections. The factor  $(1-x)$  is meant to extend the VDM contribution towards larger values of Bjorken  $x$ .

## 2.2 $\gamma^*\gamma^*$ scattering

In the same spirit, the total cross section for  $\gamma^*\gamma^*$  scattering can be written as a sum of the following five terms (see Fig.2):

$$\begin{aligned}\sigma_{\gamma^*\gamma^*}^{tot}(W, Q_1^2, Q_2^2) &= \sigma_{direct}^{tot}(W, Q_1^2, Q_2^2) + \\ &+ \sigma_{dip-dip}^{tot}(W, Q_1^2, Q_2^2) + \\ &+ \sigma_{SR1}^{tot}(W, Q_1^2, Q_2^2) + \\ &+ \sigma_{SR2}^{tot}(W, Q_1^2, Q_2^2) + \\ &+ \sigma_{DR}^{tot}(W, Q_1^2, Q_2^2).\end{aligned}\tag{5}$$

The direct term, not possible in the case of photon-proton scattering, is related to a new (as compared to the previous case) possibility of  $\gamma\gamma \rightarrow$  quark + antiquark process, and can be written formally as a sum over quark flavours

$$\sigma_{direct}^{tot}(W, Q_1^2, Q_2^2) = \sum_f \sigma_{\gamma\gamma \rightarrow q_f \bar{q}_f}(W, Q_1^2, Q_2^2). \tag{6}$$

The corresponding formulae have been known for a long time and can be found in Ref.[14].

If both photons fluctuate into perturbative quark-antiquark pairs, the interaction is due to gluonic exchanges between quarks and antiquarks represented in Fig.2 by the blob.

Formally this component can be written in terms of the photon perturbative "wave functions" and the cross section for the interaction of both dipoles

$$\begin{aligned}\sigma_{dip-dip}^{tot}(W, Q_1^2, Q_2^2) &= \sum_{a,b=1}^{N_f} \int_0^1 dz_1 \int d^2\rho_1 |\Psi_T^a(z_1, \rho_1)|^2 \\ &\cdot \int_0^1 dz_2 \int d^2\rho_2 |\Psi_T^b(z_2, \rho_2)|^2 \sigma_{dd}^{a,b}(\bar{x}_{ab}, \rho_1, \rho_2).\end{aligned}\tag{7}$$

The latter quantity is not well known. It can be easily calculated in the simplest approach of two-gluon exchange. At high energies such an approach cannot be sufficient, as gluonic ladders become essential. Due to large degree of complexity a phenomenological attitude seems indispensable. In paper [15] a new phenomenological parametrization for the azimuthal-angle averaged dipole-dipole cross section has been proposed:

$$\sigma_{dd}^{a,b}(x_{ab}, \rho_1, \rho_2) = \sigma_0^{a,b} \left[ 1 - \exp\left(-\frac{\rho_{eff}^2}{4R_0^2(x_{ab})}\right) \right] \cdot S_{thresh}(x_{ab}). \tag{8}$$

Here

$$x_{ab} = \frac{\frac{m_a^2}{z_1} + \frac{m_a^2}{1-z_1} + \frac{m_b^2}{z_2} + \frac{m_b^2}{1-z_2} + Q_1^2 + Q_2^2}{W^2 + Q_1^2 + Q_2^2} \quad (9)$$

and

$$R_0(x_{ab}) = \frac{1}{Q_0} \left( \frac{x_{ab}}{x_0} \right)^{-\lambda/2}. \quad (10)$$

Our formula for  $x_{ab}$  is different from the one used in Ref.[15]. As discussed in Ref.[3] our formula provides correct behaviour at threshold energies.

In order to take into account threshold effects for the production of  $q\bar{q}q'\bar{q}'$  an extra phenomenological function has been introduced [15]

$$S_{thresh}(x_{ab}) = (1 - x_{ab})^5 \quad (11)$$

which is set to zero if  $x_{ab} > 1$ . Different prescriptions for  $\rho_{eff}$  have been considered in Ref.[15], with  $\rho_{eff}^2 = \frac{\rho_1^2 \rho_2^2}{\rho_1^2 + \rho_2^2}$  being probably the best choice [15]. Following our philosophy of explicitly including the nonperturbative resolved photon, in photon-photon collisions completely new terms must be included (the last two diagrams in Fig.2). If one of the photons fluctuates into a quark-antiquark dipole and the second photon fluctuates into a vector meson, or vice versa, we shall call such components single resolved components. In  $\gamma\gamma$  scattering there are two such components:

$$\begin{aligned} \sigma_{SR1}^{tot}(W, Q_1^2, Q_2^2) &= \int d^2\rho_2 \int dz_2 \sum_{V_1} \frac{4\pi}{f_{V_1}^2} \left( \frac{m_{V_1}^2}{m_{V_1}^2 + Q_1^2} \right)^2 \cdot \\ &\cdot |\Psi(\rho_2, z_2, Q_2^2)|^2 \sigma_{V_1 d}^{tot}(W, Q_2^2), \end{aligned} \quad (12)$$

$$\begin{aligned} \sigma_{SR2}^{tot}(W, Q_1^2, Q_2^2) &= \int d^2\rho_1 \int dz_1 \sum_{V_2} \frac{4\pi}{f_{V_2}^2} \left( \frac{m_{V_2}^2}{m_{V_2}^2 + Q_2^2} \right)^2 \cdot \\ &\cdot |\Psi(\rho_1, z_1, Q_1^2)|^2 \sigma_{V_2 d}^{tot}(W, Q_1^2). \end{aligned} \quad (13)$$

In the formulae above:

$$\sigma_{V_i d}^{tot}(W, Q^2) = \sigma_0 \left( 1 - \exp \left( -\frac{\rho_i^2}{4R_0^2(x_g)} \right) \right) \cdot S_{thresh} \quad (14)$$

where

$$R_0(x_g) = \frac{1}{Q_0} \cdot \left( \frac{x_g}{x_0} \right)^{\lambda/2} \quad (15)$$

and, to a good approximation,

$$x_g = \frac{M_{qq}^2 + Q^2}{W^2 + Q^2} \quad (16)$$

with

$$M_{qq} = \frac{m_f^2}{z(1-z)} \quad (17)$$

where  $m_f$  is quark effective mass. In the present calculation we take  $m_f = m_0$  for  $u/\bar{u}$  and  $d/\bar{d}$  (anti)quarks and  $m_f = m_0 + 0.15$  GeV for  $s/\bar{s}$  (anti)quarks.

If each of the photons fluctuates into a vector meson the corresponding component will be called double resolved.<sup>1</sup> The corresponding cross section reads formally:

$$\begin{aligned} \sigma_{DR}^{tot}(W, Q_1^2, Q_2^2) &= \sum_{V_1 V_2} \frac{4\pi}{f_{V_1}^2} \left( \frac{m_{V_1}^2}{m_{V_1}^2 + Q_1^2} \right)^2 \cdot \\ &\cdot \frac{4\pi}{f_{V_2}^2} \left( \frac{m_{V_2}^2}{m_{V_2}^2 + Q_2^2} \right)^2 \sigma_{V_1 V_2}^{tot}(W) . \end{aligned} \quad (18)$$

The total cross section for  $V_1$ - $V_2$  scattering must be modeled. In the following we shall assume Regge factorization and use a simple parametrization which fits the world experimental data for hadron-hadron total cross sections [13]. It was demonstrated recently that in the case of the total cross sections the absorption corrections violate the factorization only marginally [17]. Assuming factorization and neglecting the off-diagonal terms due to the  $a_2$ -reggeon exchange we obtain a simple and economical form

$$\sigma_{V_1 V_2}^{tot}(W) = A_R \left( \frac{s}{s_0} \right)^{\alpha_R - 1} + A_{IP} \left( \frac{s}{s_0} \right)^{\alpha_{IP} - 1} \quad (19)$$

with  $A_R = 13.2$  mb and  $A_{IP} = 8.56$  mb,  $\alpha_R = 0.5$ ,  $\alpha_{IP} = 1.08$ ,  $s = W^2$ ,  $s_0 = 1$  GeV<sup>2</sup>.

### 3 Results

In Ref.[4] we have adjusted the parameters of our model to  $\gamma^*p$  collisions. Let us try to use these parameters to describe  $\gamma\gamma$  total cross section. In Fig.3 we present the total cross section as a function of center-of-mass energy. The

---

<sup>1</sup>In some early works in the literature this was considered as the only component to the photon-photon total cross section (see for instance [16]).

sum of all components of Fig.2 (thick-solid line) exceeds the experimental data by a factor of two or even more. The individual components are shown explicitly as well. The direct component (dash-dotted line) dominates at low energies only. At high energies the dipole-dipole (thin-solid line), single-resolved (dashed line) and double-resolved (dotted line) components are of comparable size. The overestimation of the experimental data suggests a double-counting.

Let us try to recapitulate the assumptions and/or approximations used in obtaining the formulae of the previous section. First of all it was assumed that the coupling constants responsible for the transition of photons into vector mesons are the same as those obtained from the leptonic decays of vector mesons, i.e. the on-shell approximation was used. In our case we need the corresponding coupling constants rather at  $Q^2 = 0$  and not on the meson mass shell ( $Q^2 = m_V^2$ ). In principle, there can be a weak modification by a  $Q^2$ -dependent function. We replace  $\frac{4\pi}{f_{V_i}^2} \rightarrow \frac{4\pi}{f_{V_i}^2} F_{off}(Q^2, m_{V_i}^2)$  and propose to parametrize the effect of extrapolation from meson mass shell to  $Q^2 = 0$  by means of the following form factor:

$$F_{off}(Q^2, m_{V_i}^2) = \exp \left( -\frac{(Q^2 + m_{V_i}^2)}{2\Lambda_E^2} \right). \quad (20)$$

The parameter  $\Lambda_E$  is a new nonperturbative parameter of our new model. Secondly, the “photon-wave functions” commonly used in the literature allow for large quark-antiquark dipoles. This is a nonperturbative region where the pQCD is not expected to work. Furthermore this is a region which is probably taken into account in the resolved photon components as explicit vector mesons. Therefore large-size dipoles must be removed from the photon wave functions. We propose the following modification of the “perturbative” photon wave function:

$$|\Psi(\rho, z, Q^2)|^2 \rightarrow |\Psi(\rho, z, Q^2)|^2 \exp \left( -\frac{\rho}{\rho_0} \right), \quad (21)$$

which effectively suppresses large quark-antiquark dipoles.

In the following we shall try to find the parameters  $\Lambda_E$  and  $\rho_0$  by fitting our modified model formula to the experimental data. The  $\gamma\gamma$  data is not sufficient for this purpose as different combinations of the two parameters lead to equally good description. Therefore we are forced to perform a new fit of the model parameters to both  $\gamma^*p$  and  $\gamma\gamma$  scattering.

Naively one could try to adjust the new parameters in Eq.(20) and Eq.(21) to describe the photon-photon data only. However, internal consistency would require associated modifications in  $\gamma^*p$  collisions. It is obvious that

Table 1:  $\chi^2$  in  $\gamma^*p$  scattering

		$\Lambda_E$			
		0.5	1.0	2.0	$\infty$
$\rho_0$	1.0	104.0	59.0	23.0	11.0
	2.0	51.0	22.0	4.7	2.4
	3.0	28.0	8.7	2.4	2.5
	4.0	19.0	5.0	2.3	3.0
	5.0	10.0	2.1	2.4	3.0
	6.0	7.2	1.8	2.5	3.3
	$\infty$	2.1	2.2	4.6	8.3

such modifications would destroy the nice agreement with the HERA data [18] as obtained in Ref.[4]. It becomes clear that a new simultaneous fit of the extended model to both  $\gamma^*p$  and  $\gamma\gamma$  is unavoidable. It is not clear *a priori* that a good quality fit is possible at all.

In order to quantify the quality of the simultaneous fit we propose the following simple measure of fit quality:

$$\chi_{eff}^2 = \frac{\frac{\chi_{\gamma^*p}^2}{N_{\gamma^*p}} + \frac{\chi_{\gamma\gamma}^2}{N_{\gamma\gamma}}}{2} . \quad (22)$$

This is a bit *ad hoc* statistically, but treats the  $\gamma^*p$  and  $\gamma\gamma$  processes with the same weight which seems reasonable in view of large disproportions of the  $\gamma^*p$  and  $\gamma\gamma$  data sets. In the present fit in addition to the HERA [18] data for  $\gamma^*p$  scattering we include also the PLUTO [19] and OPAL [20] collaboration data for  $\gamma\gamma$  scattering.

In Tables 1, 2 we have collected the values of minimal standard  $\chi^2$  for different pairs of the newly defined parameters of the extended model:  $\rho_0$  and  $\Lambda_E$ . Each value of  $\chi^2$  is supplemented with the values of the remaining model parameters ( $\sigma_0$ ,  $x_0$  and  $\lambda$ ) which we have not presented in the table for clarity. A rather good description of both processes can be obtained. However, the smallest values of  $\chi^2$  for both processes are situated in different parts of the two tables. In Table 3 we display the effective  $\chi^2$  defined by Eq.(22). Here the minimal value of the proposed measure  $\chi_{eff}^2$  is at  $\rho_0 = 5.0$  GeV<sup>-1</sup> and  $\Lambda_E = 1$  GeV for which  $\chi_{eff}^2 = 1.7$ .

In Fig.4 we show the resulting total cross section for the photon-photon scattering together with the experimental data of the PLUTO (solid triangles) and OPAL (open circles) collaborations. We also show the individual

Table 2:  $\chi^2$  in  $\gamma\gamma$  scattering

		$\Lambda_E$			
		0.5	1.0	2.0	$\infty$
$\rho_0$	1.0	14.0	5.2	0.7	1.2
	2.0	12.0	2.3	1.8	5.0
	3.0	9.8	1.1	4.4	8.1
	4.0	7.9	1.0	2.6	12.0
	5.0	6.8	1.6	8.9	13.0
	6.0	5.7	2.4	11.0	16.0
	$\infty$	1.5	19.0	43.0	59.0

Table 3:  $\chi^2_{eff}$  in  $\gamma^*p$  and  $\gamma\gamma$  scattering

		$\Lambda_E$			
		0.5	1.0	2.0	$\infty$
$\rho_0$	1.0	59.0	32.0	12.0	6.1
	2.0	32.0	12.0	3.3	3.7
	3.0	19.0	4.9	3.4	5.3
	4.0	14.0	3.0	2.5	7.5
	5.0	8.4	1.3	5.7	8.0
	6.0	6.5	2.1	6.5	9.7
	$\infty$	1.8	11.0	24.0	34.0



contributions of different processes from Fig.2. Please note that the relative size of the contributions has changed when compared to Fig.3. Now the sum of the so-called single resolved components dominates in the broad range of center-of-mass energies. It is worth stressing in this context that these components are included here for the first time. When compared to Fig.3 the double resolved component is now much weaker and constitutes 10-15 % of the total cross section only. For completeness in Fig.5 we show the analogous description of the  $\gamma^*p$  data. The agreement with the HERA data is similar as in our previous paper [4].

## 4 Factorization breaking

In data processing, in particular in extrapolations to small photon virtualities one often assumes the following relation

$$\sigma_{\gamma^*\gamma^*}^{tot}(W, Q_1^2, Q_2^2) = \Omega(Q_1^2) \cdot \Omega(Q_2^2) \cdot \sigma(W) \quad (23)$$

known as factorization. This relation is strictly true for single-pole double-resolved VDM components and means total decorrelation of  $Q_1^2$  and  $Q_2^2$ . In the following we shall consider two quantities which measure factorization breaking.

The first one reads

$$f_{fb}^{(1)}(W, Q_1^2, Q_2^2) \equiv \frac{\sigma_{\gamma^*\gamma^*}(W, Q_1^2, 0) \sigma_{\gamma^*\gamma^*}(W, 0, Q_2^2)}{\sigma_{\gamma^*\gamma^*}(W, Q_1^2, Q_2^2) \sigma_{\gamma^*\gamma^*}(W, 0, 0)} . \quad (24)$$

For the factorized Ansatz (23)  $f_{fb}^{(1)} = 1$ . This quantity may be difficult to measure at present as it requires knowledge of the cross section for real photons, which is not possible with present  $e^+e^-$  colliders and the detectors used. We hope this quantity can be used in the future with the help of the photon-photon option at TESLA [21].

The second quantity <sup>2</sup> is

$$f_{fb}^{(2)}(W, Q_1^2, Q_2^2) \equiv \frac{\sigma_{\gamma^*\gamma^*}(W, Q_1^2, Q_1^2) \sigma_{\gamma^*\gamma^*}(W, Q_2^2, Q_2^2)}{\sigma_{\gamma^*\gamma^*}(W, Q_1^2, Q_2^2) \sigma_{\gamma^*\gamma^*}(W, Q_2^2, Q_1^2)} . \quad (25)$$

As in the previous case it is easy to check that with the factorized Ansatz (23)  $f_{fb}^{(2)} = 1$ . The effect of factorization breaking is limited through the following normalization condition

$$f_{fb}^{(2)}(W, Q^2, Q^2) = 1 . \quad (26)$$

---

<sup>2</sup>A similar quantity has been used to study factorization breaking of a color dipole BFKL approach [22] to highly virtual photon - highly virtual photon scattering

Therefore it becomes clear that this quantity becomes interesting if  $Q_1^2 \gg Q_2^2$  or  $Q_1^2 \ll Q_2^2$ . The second quantity measures formally (de)correlations of both photons virtualities. In principle, this quantity can be used in the analysis of existing experimental data from DESY, SLAC or LEP.

Both quantities proposed for measuring factorization breaking require knowledge of the total cross section not only for the real photons but also for the virtual ones. Before we present the quantities in question we wish to display the total photon-photon cross section as a function of both photon virtualities. In Fig.6 we show the corresponding maps for two quite different energies  $W = 10$  GeV and  $W = 100$  GeV in measurable range of photon virtualities. Two observations can be made here. First, the two maps look rather similar. Secondly, fast fall-off is observed at photon virtualities  $0 < Q^2 < 1$  GeV<sup>2</sup>, with further decrease being much softer.

The factorization-breaking function  $f_{fb}^{(1)}$  is shown in Fig.7 as a function of both photon virtualities  $Q_1^2$  and  $Q_2^2$  for  $W = 10$  GeV (left panel) and  $W = 100$  GeV (right panel). According to the definition (24) at  $Q_1^2 = 0$  or  $Q_2^2 = 0$  we have  $f_{fb}^{(1)} = 1$ . The rapid variation of the function is not best represented by our rough grid. For completeness the second proposed function is shown in Fig.8. By definition this time (see Eq.(25)) we have  $f_{fb}^{(2)} = 1$  when  $Q_1^2 = Q_2^2$ . As in the previous case fast variation occurs at small photon virtualities.

Having understood the general behaviour we wish to focus on the most interesting parts of the  $(Q_1^2, Q_2^2)$  space. In Fig.9 we show the behaviour of the two-dimensional function  $f_{fb}^{(1)}(Q_1^2, Q_2^2)$  along the diagonal  $Q^2 = Q_1^2 = Q_2^2$  and in Fig.10  $f_{fb}^{(2)}(0, Q^2) = f_{fb}^{(2)}(Q^2, 0)$  along the line  $Q^2 = Q_2^2$  ( $Q_1^2 = 0$ ). The thick solid line represents our full model with all components included. For illustration we have shown also factorization breaking functions for separate mechanisms (components in the expansion (5)). Quite a different behaviour can be observed for different mechanisms. Let us concentrate first on the  $f_{fb}^{(1)}$  function. While the single resolved and direct component grow with  $Q^2$  the dipole-dipole component decreases. Paradoxically, the total  $f_{fb}^{(1)}$  is smaller than the one for the dipole-dipole component. This surprising result is related to the nonlinearity of the quite complicated function  $f_{fb}^{(1)}(Q^2, Q^2)$  which in fact involves four correlated points in the  $(Q_1^2, Q_2^2)$  plane. A completely reverse behaviour can be seen for  $f_{fb}^{(2)}$ . This has a simple analytic explanation. Substituting  $Q_1^2 = Q^2$  and  $Q_2^2 = Q^2$  into Eq.(24) and  $Q_1^2 = 0$  and  $Q_2^2 = Q^2$  or  $Q_1^2 = Q^2$  and  $Q_2^2 = 0$  into Eq.(25) we find:

$$f_{fb}^{(1)}(W, Q^2, Q^2) = \frac{1}{f_{fb}^{(2)}(W, 0, Q^2)} = \frac{1}{f_{fb}^{(2)}(W, Q^2, 0)}. \quad (27)$$

## 5 Conclusions

In our former paper we have constructed a simple model for  $\gamma^*p$  total cross section which, in contrast to other models in the literature, includes the resolved photon component. The latter is known to be the necessary ingredient when discussing exclusive reactions. In the present paper we have generalized the model to the case of  $\gamma\gamma$  scattering. In the last case a few new components appear so far not discussed in the literature.

The naive generalization of our former model for  $\gamma^*p$  total cross section leads to a serious overestimation of the  $\gamma\gamma$  total cross sections. In general, this fact can be due either to a nonoptimal set of model parameters found in our previous study or/and due to some model simplifications. For instance, it is customary that model parameters for resolved photon component obtained in the vector meson dominance approach are taken from vector meson dileptonic decays, i.e. on meson mass shell. In the  $\gamma^*p$  and  $\gamma\gamma$  processes, of interest to us, vector mesons are rather off-shell. Therefore one could expect some off-shell effects. Calculating such off-shell effects in nonelementary processes is not a simple task. In this paper we have suggested to include such an effect by introducing new form factors which we call off-shell form factors for simplicity. On the other hand, when including the quark-antiquark continuum one usually takes into account the perturbative quark-antiquark "photon wave function". This is justified and reasonable for small size dipoles only. The physics of large-size dipoles must involve nonperturbative effects which may lead to double counting in our model. In order to avoid double counting the large-size dipoles must be eliminated. We reduce their contribution using a simple exponential function in transverse dipole size. Summarizing, the two new functions bring in two new model parameters. Having this freedom we have performed a new fit of our generalized-model parameters to the  $\gamma^*p$  and  $\gamma\gamma$  experimental data. The generalization of the model for meson off-shell effects and large dipole size effects discussed above permits a simultaneous description of both processes considered.

When trying to extrapolate the experimental cross sections for the  $\gamma^*\gamma^*$  scattering to real photons one often assumes factorization. Our multicomponent model violates this assumption. We have quantified the effects of factorization breaking in our model with parameters fixed to describe the  $\gamma^*p$  and  $\gamma\gamma$  data. We have proposed two functions which can be used as a measure of factorization breaking. We have found a strong effect, rather weakly dependent of the center of mass  $\gamma^*\gamma^*$  energy. Experimental search of such effects could teach us more about reaction mechanism. Certainly, it is not an easy task with the LEP2 apparatus.

**Acknowledgments** We are indebted to Mariusz Przybycień from the OPAL collaboration for an interesting discussion.

## References

- [1] K. Golec-Biernat and M. Wüsthoff, Phys. Rev. **D60** (1999) 114023-1.
- [2] J. Breitweg et al. (ZEUS collaboration), Phys. Lett. **B479** (2000) 37.
- [3] A. Szczurek, Eur. Phys. J. **C26**, (2002) 183.
- [4] T. Pietrycki, A. Szczurek, Eur. Phys. J. **C31**, (2003) 379.
- [5] K. Golec-Biernat and M. Wüsthoff, Phys. Rev. **D59** (1999) 014017.
- [6] J.R. Forshaw, G. Kerley and G. Shaw, Phys. Rev. **D60** (1999) 074012.
- [7] G.R. Kerley and McDermott, J. Phys. **G26** (2000) 683.
- [8] A.D. Martin, M.G. Ryskin and A.M. Staśto, Eur. Phys. J. **C7** (1999) 643.
- [9] E. Gotsman, E. Levin, U. Maor and E. Naftali, Eur. Phys. J. **C10** (1999) 689.
- [10] G.A. Schuler and T. Sjöstrand, Z. Phys. **C73** (1997) 677.
- [11] E.V. Bugaev, Yu.V. Shlepin, Phys. Rev. **D67** (2003) 034027.
- [12] A. Szczurek and V. Uleshchenko, Eur. Phys. J. **C12** (2000) 663.
- [13] A. Donachie, P.V. Landshoff, Phys. Lett. **B296**, (1992) 227.
- [14] V.M. Budnev, I.F. Ginzburg, G.V. Meledin and V.G. Serbo, Phys. Rep. **C15** (1975) 181.
- [15] N. Timneanu, J. Kwieciński and L. Motyka, Eur. Phys. J. **C23** (2002) 513.
- [16] I.F. Ginzburg and V.G. Serbo, Phys. Lett. **B109** (1982) 231.
- [17] A. Szczurek, N.N. Nikolaev and J. Speth, Phys. Rev. **C66** (2002) 055206.
- [18] J. Breitweg et al.(ZEUS collaboration), Phys. Lett. B **487**, (2000) 53; S. Chekanov et al.(ZEUS collaboration), preprint DESY-01-064; C. Adloff et al.(H1 collaboration), Eur. Phys. J. C **21**, (2001) 33.

- [19] Ch. Berger et al.(PLUTO collaboration), Phys. Lett. **B149** (1984) 421.
- [20] S. Abbiendi et al.(OPAL collaboration), Eur. Phys. J. **C14** (2000) 199.
- [21] TESLA Technical Design Report, PART VI, Chapter 1: The Photon Collider at TESLA, Int. J. Mod. Phys. **A19** (2004) 5097.
- [22] N.N. Nikolaev, J. Speth and V.R. Zoller, Eur. Phys. J. **C22** (2002) 637.

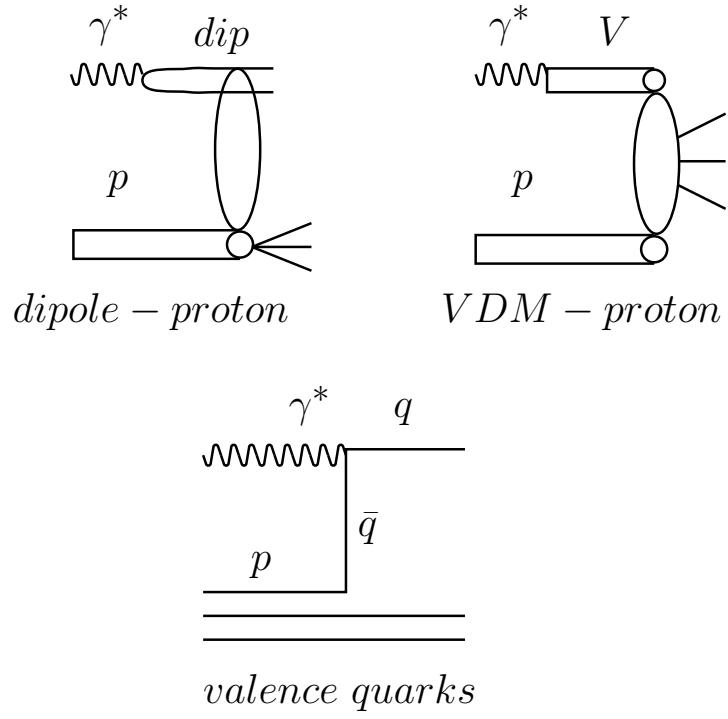


Figure 1: *The graphical illustration of the multicomponent  $\gamma^* p$  scattering model.*

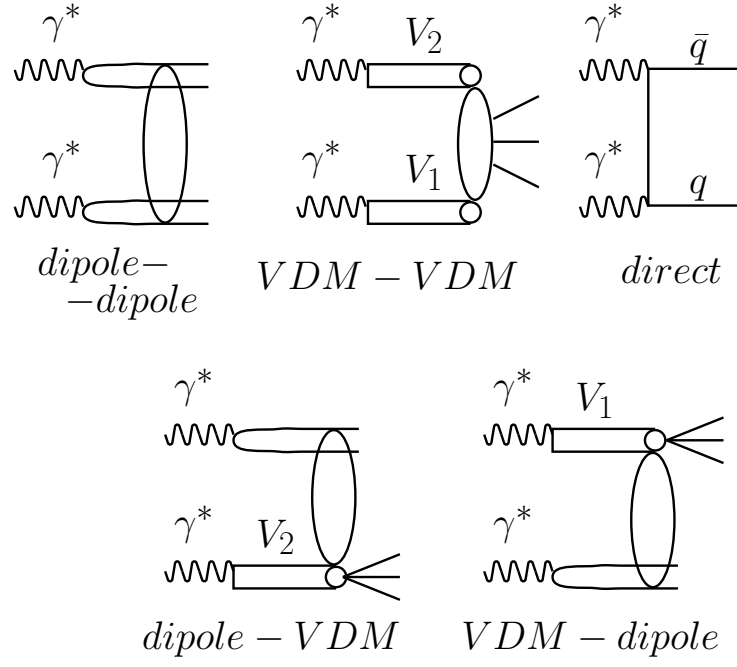


Figure 2: The graphical illustration of the multicomponent  $\gamma^*\gamma^*$  scattering model.

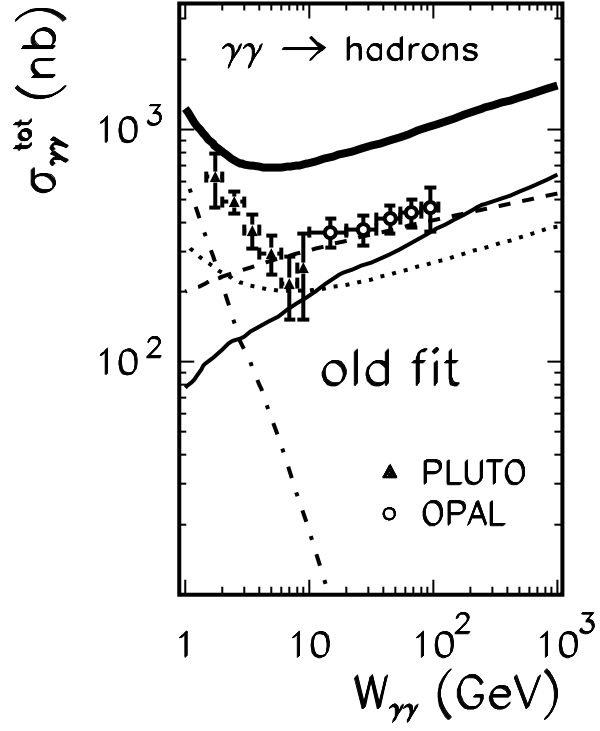


Figure 3: *The total  $\gamma\gamma$  cross section as a function of photon-photon energy with parameters from Ref.[4]. The experimental data are from [19, 20].*



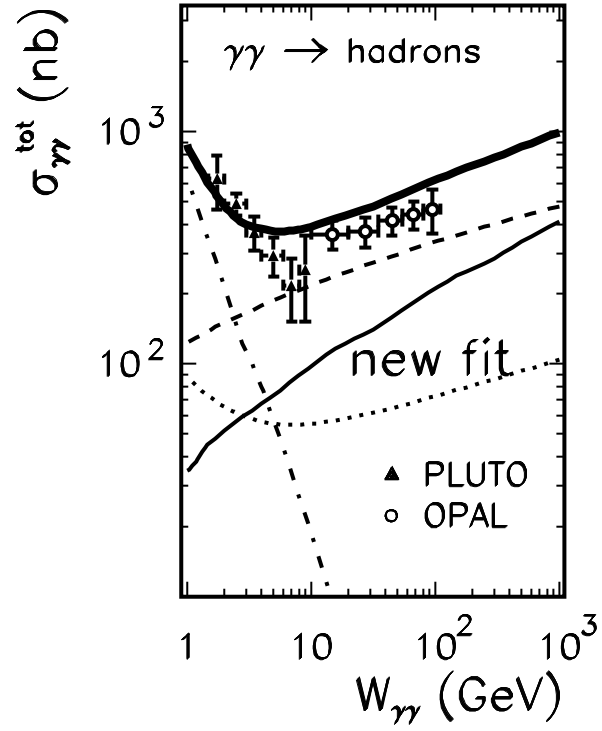


Figure 4: *The total  $\gamma\gamma$  cross section as a function of photon-photon energy with the new set of parameters. The experimental data are from [19, 20].*

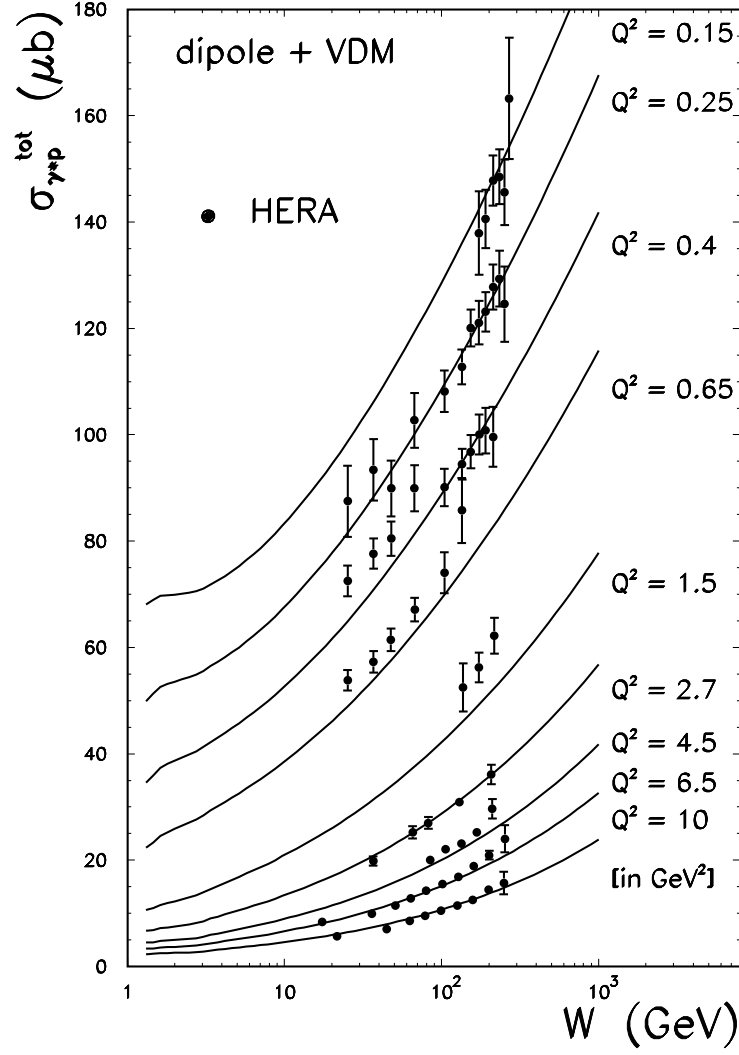
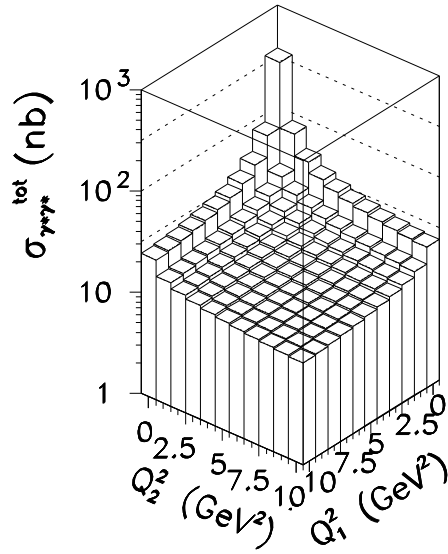
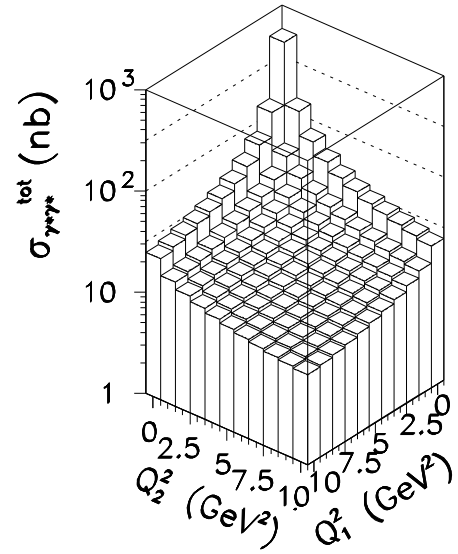


Figure 5: The total  $\gamma^*p$  cross section as a function of photon-proton energy. The experimental HERA data are from [18].

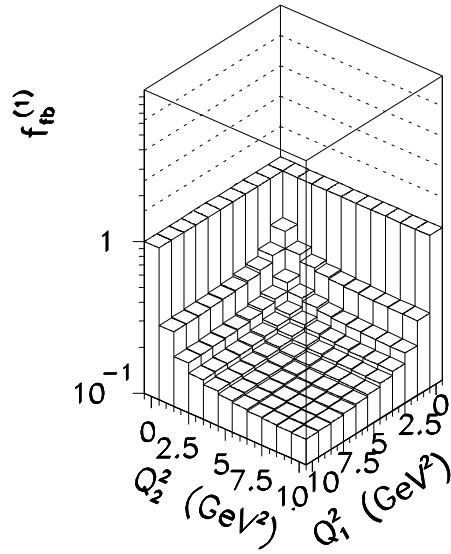


(a)

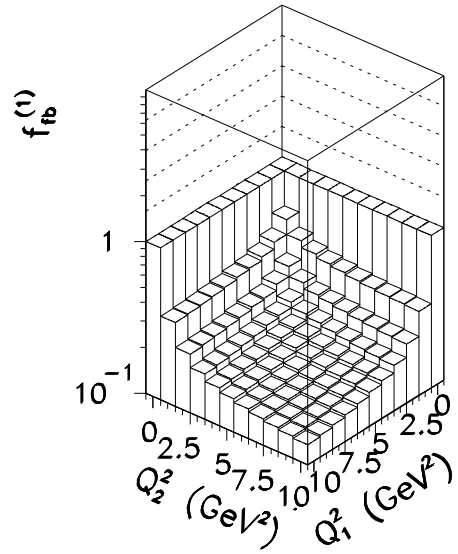


(b)

Figure 6: *The maps of the total  $\gamma^*\gamma^*$  cross section as a function of both photon virtualities  $Q_1^2$  and  $Q_2^2$  for  $W = 10$  GeV (left panel) and  $W = 100$  GeV (right panel).*



(a)



(b)

Figure 7: The maps of the factorization-breaking function  $f_{fb}^{(1)}$  as a function of both photon virtualities  $Q_1^2$  and  $Q_2^2$  for  $W = 10$  GeV (left panel) and  $W = 100$  GeV (right panel).

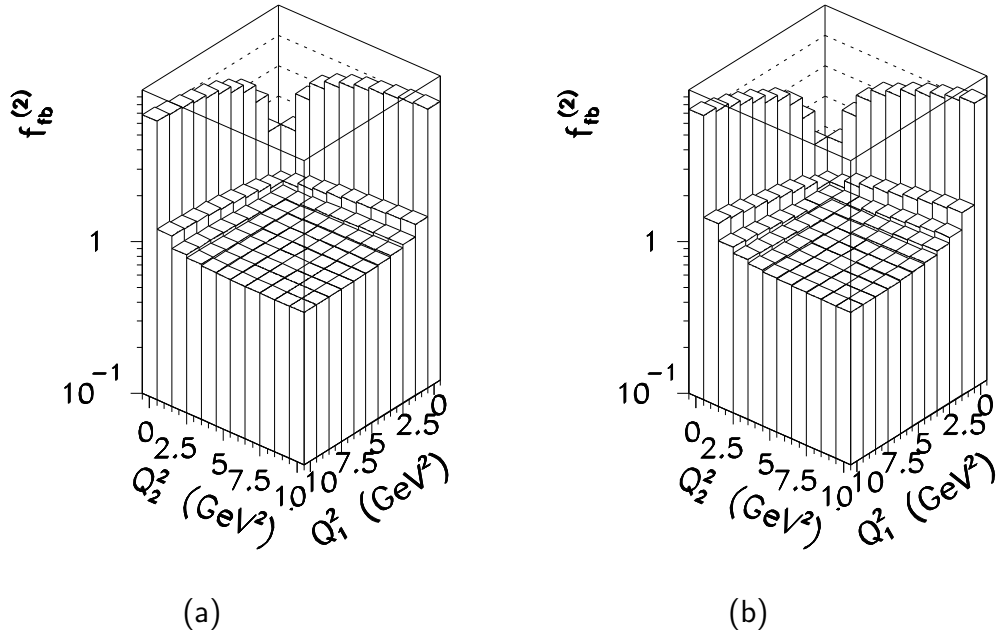


Figure 8: The maps of the factorization-breaking function  $f_{fb}^{(2)}$  as a function of both photon virtualities  $Q_1^2$  and  $Q_2^2$  for  $W = 10$  GeV (left panel) and  $W = 100$  GeV (right panel).

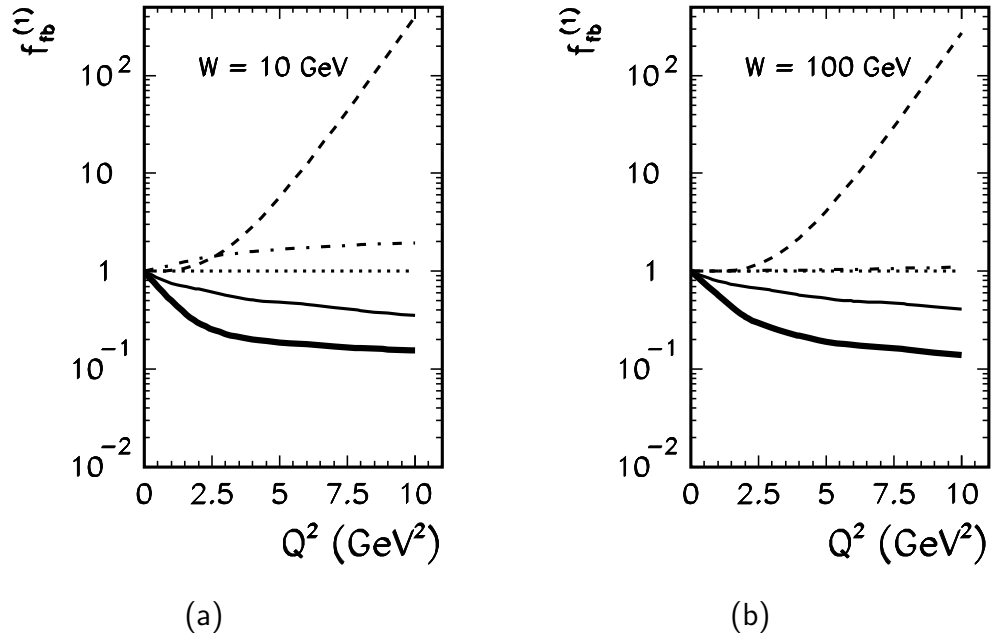
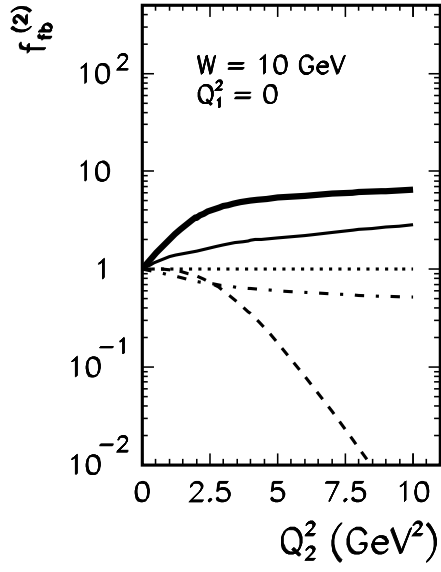
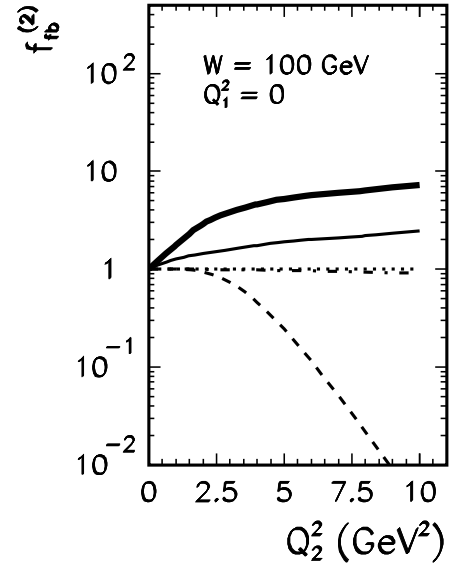


Figure 9: Factorization breaking function  $f_{fb}^{(1)}$  as a function of  $Q^2$  ( $Q^2 = Q_1^2 = Q_2^2$ ) for  $W = 10 \text{ GeV}$  (left panel) and  $W = 100 \text{ GeV}$  (right panel).



(a)



(b)

Figure 10: Factorization breaking function  $f_{fb}^{(2)}$  as a function of  $Q_2^2$  ( $Q_1^2 = 0$ ) for  $W = 10$  GeV (left panel) and  $W = 100$  GeV (right panel).